DOI: 10.1002/chem.200801775

Regioselective Reactivity of an Asymmetric Tetravalent Di[dihydroxotin(IV)] Bis-Porphyrin Host Driven by Hydrogen-Bond Templation

Peter R. Brotherhood, Ian J. Luck, Iain M. Blake, Paul Jensen, Peter Turner, and Maxwell J. Crossley*[a]

Abstract: Local molecular environment effects on the rates of ligand exchange at an asymmetric di[dihydroxotin(IV)] bis-porphyrin **5** are examined. The host **5** possesses four non-equivalent tin(IV)–ligand binding sites that are distinguished by their position relative to a shallow cavity, by the steric environment at each binding site and by electronic-structure differences between the constituent porphyrin and quinoxalinoporphyrin macrocycles. These design features of the asymmetric host are confirmed by X-ray crystal structure analysis. Binding experiments with monodentate carboxylic acids and bidentate dicarboxylic acids show significant differences in the rate of ligand exchange at each of the four tin(IV) binding sites. For monodentate carboxylic acids, binding preferentially occurs at the exterior porphyrin site. Further addition of carboxylic acid results in sequential binding at the quinoxalinoporphyrin sites and lastly at the interior site on the porphyrin, with high regioselectivity. These selective binding outcomes are immediately apparent by NMR spectroscopy. A series of 2D NMR spectroscopy experiments allowed identification of the preferred binding sites at the host. This positively identifies that steric hindrance and electron-withdrawing functionality on the porphyrin macrocycle impede ligand exchange. However, these effects are overcome by dicarboxylic acid guests, which form ditopic hydrogen-bond interactions between the intracavity hydroxo ligands in the initial stage of ligand exchange, leading to regioselective binding between the tin(IV) sites within the cavity. It is envisaged that the factors identified herein that define regioselective ligand exchange at host **5** will find wider application in supramolecular systems incorporating tin(IV) porphyrins.

Keywords: host–guest systems · NMR spectroscopy · porphyrinoids · supramolecular chemistry · Tröger's base

Introduction

Biological systems are adept in the use of labile interactions to define selectivity in molecular interactions through equilibration to a thermodynamically or kinetically stable conformation.[1] These conformations are often then stabilised by the formation of covalent bonds between assembled components. Stabilisation of protein quaternary structure by disulfide bonds is an obvious example.[2] Mimicry of biological assembly phenomena in artificial supramolecular systems has afforded many structures that have strong potential for application in technology. As in nature, artificial systems are assembled with selectivity that is dictated by thermodynamic control. Multiple labile forces between components may act in concert to define the assembly outcome,[3] or conditions are employed under which covalent bond formation between components is reversible.[4] The topic of this paper, ligand exchange chemistry of dihydroxotin(IV) porphyrins, is a system that offers the potential to use both labile interaction to define selective assembly of components and, ultimately, covalent strength association of components.[5]

Tin(IV) porphyrins have been used in supramolecular chemistry due to their spontaneous, chemoselective, covalent strength binding of oxyanions at the six-coordinate tin(IV) metal centre.[6–9] Many examples also utilise the interesting optical and electronic properties of the tin(IV) porphyrin.[10] These studies have largely generated complexes

[a] P. R. Brotherhood, Dr. I. J. Luck, Dr. I. M. Blake, Dr. P. Jensen, Dr. P. Turner, Prof. M. J. Crossley
School of Chemistry, F11
The University of Sydney, NSW 2006 (Australia)
Fax: (+61) 2-9351-3329
E-mail: m.crossley@chem.usyd.edu.au

Supporting information for this article is available on the WWW under http://dx.doi.org/10.1002/chem.200801775.

with symmetric axial ligation about the six-coordinate tin(IV) metal centre.

Ligand exchange at dihydroxotin(IV) porphyrins proceeds by initial outer-sphere hydrogen-bond equilibrium between an incoming protic oxygen molecule (typically a carboxylic acid) and the oxygen of the bound hydroxo ligand.[5–8,11] Subsequently, the protonated hydroxo ligand (water) dissociates and the carboxylate anion may then associate by an ester-like bond at the tin(IV) centre. Once bound at the tin(IV) centre, carboxylate ligands tend only to exchange in the presence of free acid of comparable or greater strength than that bound.[11,12] It is the initial hydrogen-bond equilibrium that offers the potential for kinetic or thermodynamic control over the site of interaction of the carboxylic acid with the dihydroxotin(IV) porphyrin host.

Herein we describe the design, synthesis and crystallographic characterisation of an asymmetric tetravalent di[dihydroxotin(IV)] bis-porphyrin host molecule **5** that possesses four non-equivalent binding sites, and binding studies with this host and carboxylic acids. These allow us to identify factors that are symptomatic of the host asymmetry, and that result in the highly regioselective binding of carboxylate anions at specific sites on host **5**. This work identifies factors that may be utilised to control facial selectivity in ligand exchange at tin(IV) porphyrins, expanding their utility in supramolecular chemistry.

Results and Discussion

Synthesis and crystal structure analysis of asymmetric host 5: The precursor to host **5**, free-base, asymmetric bis-porphyrin **4**, was synthesised by the acid-catalysed condensation of the 2-aminoporphyrin **1** and the aminoquinoxalinoporphyrin **2** with formaldehyde (Scheme 1).[13–15] A two molar equivalent excess of the less-reactive **1** was employed. The three major products from the crude reaction mixture could be isolated by chromatography over silica gel and separation was best achieved as their dizinc(II) chelates. The homo-coupled dizinc(II) Tröger's base bis-porphyrin[16] was isolated in 52% yield and extended dizinc(II) Tröger's base bis-quinoxalinoporphyrin[14,17] was obtained in 48% yield. Once isolated, dizinc(II) asymmetric bis-porphyrin **3** was demetallated by treatment with hydrochloric acid to yield the free-base asymmetric bis-porphyrin **4** in 14% overall yield from **2**.

Formation of the asymmetric bis-porphyrin product demonstrates the applicability of the Tröger's base reaction to the cross-condensation of arylamines of quite different electronic structures, in this case a macrocyclic heteroaromatic amine **1** and an aromatic fused aniline **2**.[18] This reaction, in a single step, has also imparted asymmetry, chirality, concavity and rigidity on the host framework.

Free-base asymmetric bis-porphyrin **4** was then treated with tin(II) chloride in pyridine at reflux,[19,20] and hydrolysed to di[dihydroxotin(IV)] host **5** in 80% yield by heating at reflux in 4:1 tetrahydrofuran/aqueous potassium carbonate,[21] see Scheme 1. ^{1}H NMR and high-resolution electrospray ionisation Fourier transform ion cyclotron resonance (HR-ESI-FT/ICR) spectra for **3**, **4** and **5** are provided in the Supporting Information. Recrystallisation of **5** from dichloromethane/acetonitrile yielded crystals suitable for X-ray crystal structure analysis.

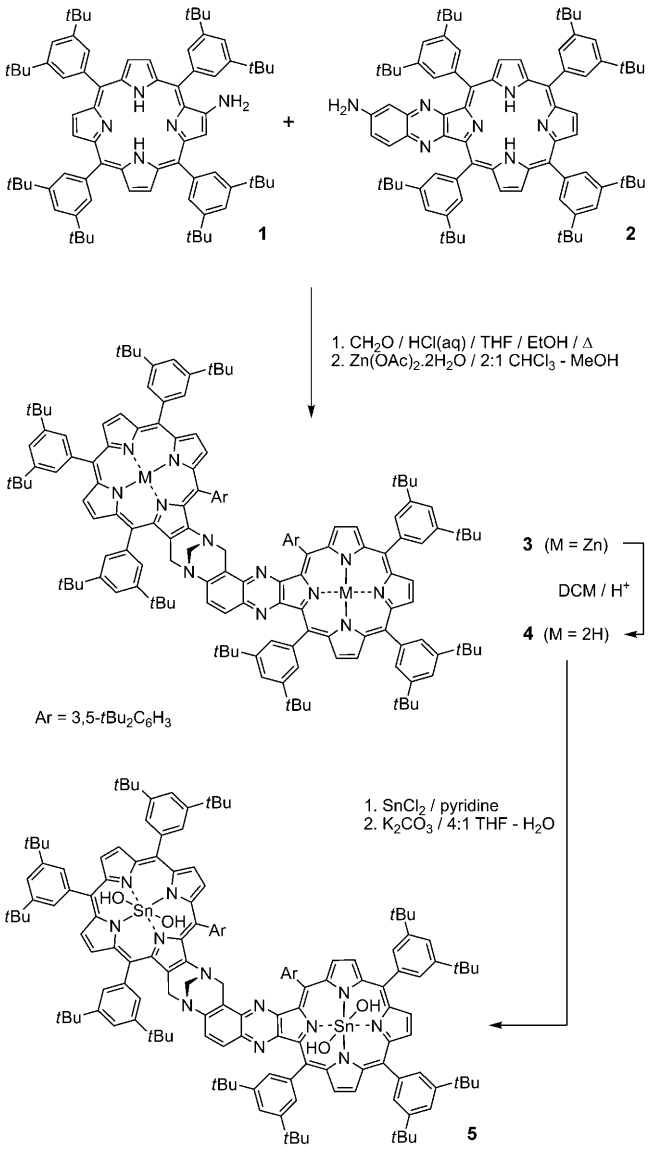

Scheme 1. Synthesis of di[dihydroxotin(IV)] asymmetric host **5**.

Crystal structure analysis allows identification of many of the design features of host **5**, depicted in Figure 1. The asymmetric surface is immediately evident. The concavity imparted by the methanodiazocine Tröger's base bridge results in the formation of a shallow cavity at one face of the host, into which two of the hydroxo-ligand–carboxylate interaction sites project. The remaining two binding sites of the host, one on the porphyrin and one on the quinoxalinoporphyrin, project outwards from the exterior of the cavity. The distance between the tin(IV) metal centres across the interior of the cavity is 12.8 Å, which is sufficient to allow

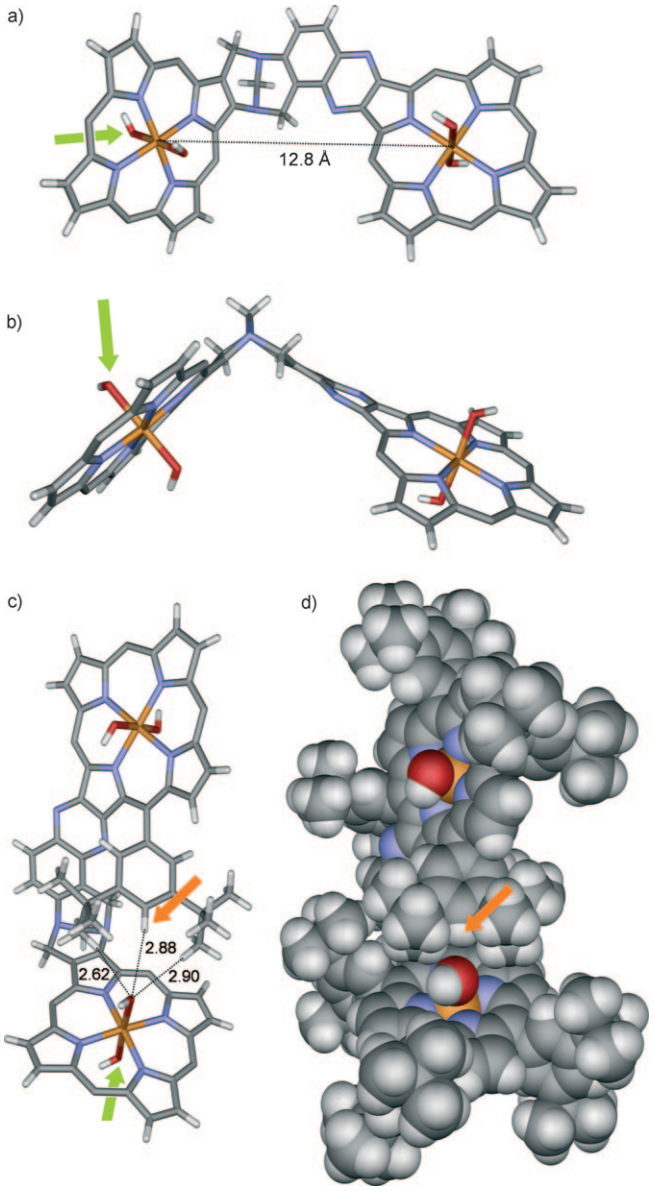

Figure 1. X-ray crystal structure of **5**. Distances are given in Å. a) View into the cavity. b) Side view, (3,5-tBu$_2$C$_6$H$_3$ groups removed for clarity). c) View into the cavity showing the proximity of the cavity aryl group to the hydroxo ligand at the interior face of the porphyrin. d) Full structure (solvent and disorder removed) view into cavity. The cavity aryl proton is indicated with the orange arrows. The "preferred" site of ligand exchange at $\leq$1 molar equivalents monodentate guest (identified by NMR spectroscopy) is indicated by the green arrows.

the ditopic binding of aliphatic dicarboxylic acids in the order of six to ten carbons in length.[22] Note the steric environment about these intracavity binding sites. In the solid state, the binding sites at the interior and exterior face of the quinoxalinoporphyrin and at the exterior face of the porphyrin are sterically unencumbered. The binding site at the interior face of the porphyrin, however, is obscured from one side by a 3,5-di-*tert*-butylphenyl group appended at a *meso* position of the quinoxalinoporphyrin. This arrangement is indicated in Figure 1c and d. Indeed, the *para*-aryl proton on this *meso*-aryl substituent to the quinoxalinoporphyrin, hereafter referred to as the cavity aryl proton (indicated by the orange arrows in Figure 1), resonates characteristically upfield at $\delta = 5.99$ ppm, confirming its orientation in close proximity to the shielding effect of the porphyrin macrocycle. Only protons in close vertical proximity above or below the plane of the porphyrin macrocycle fall within this shielding zone.[23] The other aryl protons on **5** resonate between $\delta = 7.59$ and 8.32 ppm. The cavity aryl proton resonates at even higher field in the free-base **4** and dizinc(II) analogues of host **5**, at $\delta = 5.15$ and 4.96 ppm, respectively (see Figures S1 and S3 in the Supporting Information).

As well as the steric and cavity influences on the tin(IV) ligation sites identified by crystallography, there are known electronic-structure differences between the porphyrin macrocycle and the quinoxalinoporphyrin macrocycle that may affect the rate of ligand exchange at each tin(IV) metal centre. It is known from the electrochemistry of monomeric quinoxalinoporphyrins that the addition of the quinoxalino group activates the reduction of the porphyrin macrocycle and the reduction of electroactive metal centres bound at the inner periphery.[18,24] These electronic effects may also influence the strength of tin(IV)–hydroxo bonds, the basicity of the hydroxo oxygen, and its capacity to accept hydrogen bonds from incoming carboxylic acid guests, thereby slowing the rate of ligand exchange at the quinoxalinoporphyrin macrocycle compared with the rate of exchange at the porphyrin. We describe experiments designed to test this hypothesis later in the discussion.

These factors, the presence of a shallow cavity, the steric environment at each of the binding sites and the electronic differences between the two macrocycles, operate in concert such that there are significant differences in the propensity of ligand exchange at each of these four sites. The experiments subsequently described in this paper identify the operation of these factors in leading to regioselective ligand exchange at **5**. We have identified, by NMR spectroscopy, the preferred site for ligand exchange as being on the exterior of the porphyrin macrocycle (indicated by the green arrows in Figure 1a and b) and positively identified the factors that lead to binding regioselectivity.

Binding studies with monodentate carboxylic acids: Formic acid (**6**), acetic acid (**7**) and pivalic acid (**8**) were selected for their variation in steric demand immediately about the carboxylate functionality. When these acids are introduced independently to host **5** in $\leq$1 molar equivalent aliquots, ligand exchange occurs primarily at only one of the four sites on the host, to form new dihydroxotin(IV)–carboxylatohydroxotin(IV) complexes **5·6**, **5·7** and **5·8** in 60–80% yield, depending on the carboxylic acid used. The remaining carboxylic acid binds to the host in a random fashion, either to form other 1:1 complexes or complexes with higher carboxylate/**5** ratios. At the completion of binding no free carboxylic acid is detected.

^{1}H–^{119}Sn HMQC provides major evidence that regioselective ligand exchange occurs at only one of the four binding

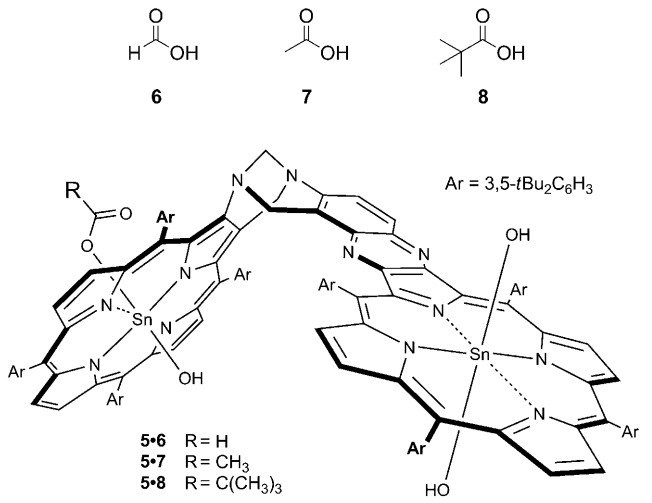

sites on host **5** with the initial ≤ 1 molar equivalent aliquot of carboxylic acid guest. The ^{119}Sn chemical shift is sensitive to the functionality of the porphyrin macrocycle and to the nature of axial ligation and there are characteristic chemical shift ranges for dihydroxotin(IV) nuclei, hydroxocarboxylatotin(IV) nuclei and dicarboxylatotin(IV) nuclei.[25] The ^{1}H–^{119}Sn HMQC for complex **5•7**, depicted in Figure 2a, identifies the β-pyrrolic resonances and the acetate resonance corresponding to the hydroxoacetato ^{119}Sn nucleus and confirms the assignment of the initial site of ligand exchange discussed below.

Regioselective binding is also evident by 1D ^{1}H NMR spectroscopy. There are three regions of the ^{1}H NMR spectrum in which this is most easily identified: the methanodiazocine bridge resonances ($\delta = 4$ to 5 ppm), the resonance for the cavity aryl proton ($\delta = 6$ to 7 ppm), identified in Figure 1, and the resonance for the bound ligand ($\delta = 0$ to -2 ppm). The protons in each of these environments are particularly sensitive to changes in the pattern of ligation about the host and dispersion of these signals is good, allowing identification of signals due to new complexes. ^{1}H NMR spectra for complexes **5•6**, **5•7** and **5•8** show six new doublets in the methanodiazocine bridge region and a single new resonance for the cavity aryl proton. For **5•7** and **5•8**, single carboxylate ligand environments are apparent at $\delta = -1.15$ and -1.30 ppm, respectively. The bound formate resonance for **5•6** coincides with the *tert*-butyl proton resonances. These ^{1}H NMR spectra are shown in Figure S6 in the Supporting Information.

An important control experiment is one in which the outcome of random ligand exchange is examined. An addition of 1 to ≤ 3 molar equivalents of **7** results in formation of many complexes resulting from non-selective ligand exchange at the three remaining sites on the host once binding is complete at the first, "preferred" site. The ^{1}H NMR spectra for mixtures of complexes thus generated are too complicated to interpret and the ^{1}H–^{119}Sn HMQC at two molar equivalents of **7** shows many ^{119}Sn environments, see Figures S7 and S8 in the Supporting Information.

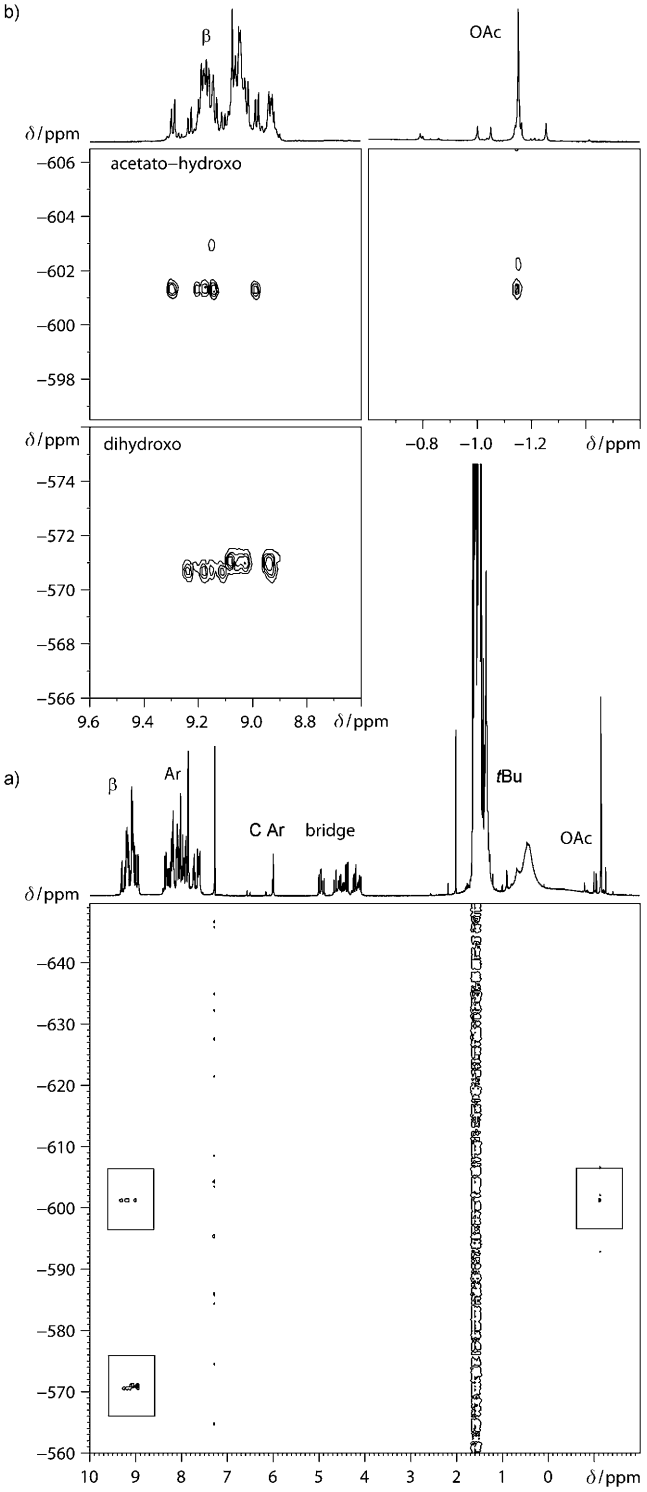

Figure 2. NMR spectroscopy characterisation of regioselective 1:1 acetate binding at host **5**. a) Complete ^{1}H–^{119}Sn HMQC (400 MHz, $CDCl_3$, 300 K) of host **5**+0.95 molar equivalents acetic acid **7** (**5•7**). Note the presence of only one new hydroxoacetatotin(IV) environment (^{119}Sn$\delta = -601$ ppm). C Ar indicates the signal for the cavity aryl proton defined in Figure 1. b) Expansion of boxed regions in a.

These titration experiments demonstrate regioselective ligand exchange upon addition of ≤ 1 molar equivalent of **6**,

7 or **8** to host **5**. These results show that the morphology of host **5** and the electronic effects at each macrocycle act to direct ligand exchange preferentially to only one of the four binding sites. The next sections are devoted to identification of the preferred binding site and the factors that are important in its selection.

Identification of the preferred binding site by NMR: Detection of NOE and through-bond interactions[9a,b] between the nuclei of bound **7** and **8** in complexes **5·7** and **5·8**, and the nuclei of the host framework, allow paths of connectivity to be established such that the initial site of ligand exchange can be identified. During the course of these investigations, we also made a full ^{1}H and ^{119}Sn NMR assignment for host **5** and its di[diacetatotin(IV)] complex.[26] Identical pathways exist in these complexes to those that allow the assignment of **5·7** and **5·8**.

The experiments used to identify these paths of connectivity in host **5** and the carboxylate complexes were NOESY, ROESY employing varied mixing times, double quantum filtered correlation spectroscopy (DQF-COSY), ^{1}H–^{119}Sn HMQC, ^{1}H–^{13}C HMBC and ^{1}H–^{13}C HSQC. For these experiments, **5·7** and **5·8** were generated by adding 0.9 molar equivalents of **7** and 0.7 molar equivalents **8**, respectively. It was found that the ROESY experiments gave better results at lower temperature. The spectra discussed in this section were obtained at 250 K, after sufficient time at room temperature was allowed for binding to go to completion.

For **5·7** and **5·8**, two paths of NOE and through-bond connectivity were identified, which show that the preferred site of exchange at ≤ 1 molar equivalent of guest is at the exterior cavity position of the porphyrin macrocycle (this position is indicated in Figure 1 by the green arrows). The first of these paths is shown in Figure 3 by the red arrows. In Figure 3a the bound ligand is **7**, however, this connectivity was also established for **5·8**. The quinoxalino proton adjacent to the methanodiazocine bridge is the "anchor" in the framework of host **5** to which the position of the bound ligand can be tied. This quinoxalino proton experiences NOE interaction (interaction 1 (red) in Figure 3) with one of the bridge methylene protons. This bridge proton couples with its partner on the same carbon (interaction 2 (red) in Figure 3), which in turn connects through space to an *ortho* proton of a *meso*-aryl group on the porphyrin macrocycle (interaction 3 (red) in Figure 3). This pathway establishes the position of this *ortho* aryl proton as being exterior to the cavity of host **5**. This aryl proton then connects (interaction 4 in Figure 3) through NOE to the bound ligand protons. Further evidence for the facial assignment comes from the connectivity (interactions A and B in Figure 3) between the endocyclic bridge methylene proton and the *ortho*-aryl proton projecting into the cavity (interaction A in Figure 3). Coupling of the interior cavity and exterior cavity *ortho* protons (interaction B in Figure 3) was detected by DQF-COSY and ^{1}H–^{13}C HMBC.

The second path of connectivity defining the initial site of complexation for **5·7** and **5·8** is indicated by the blue arrows

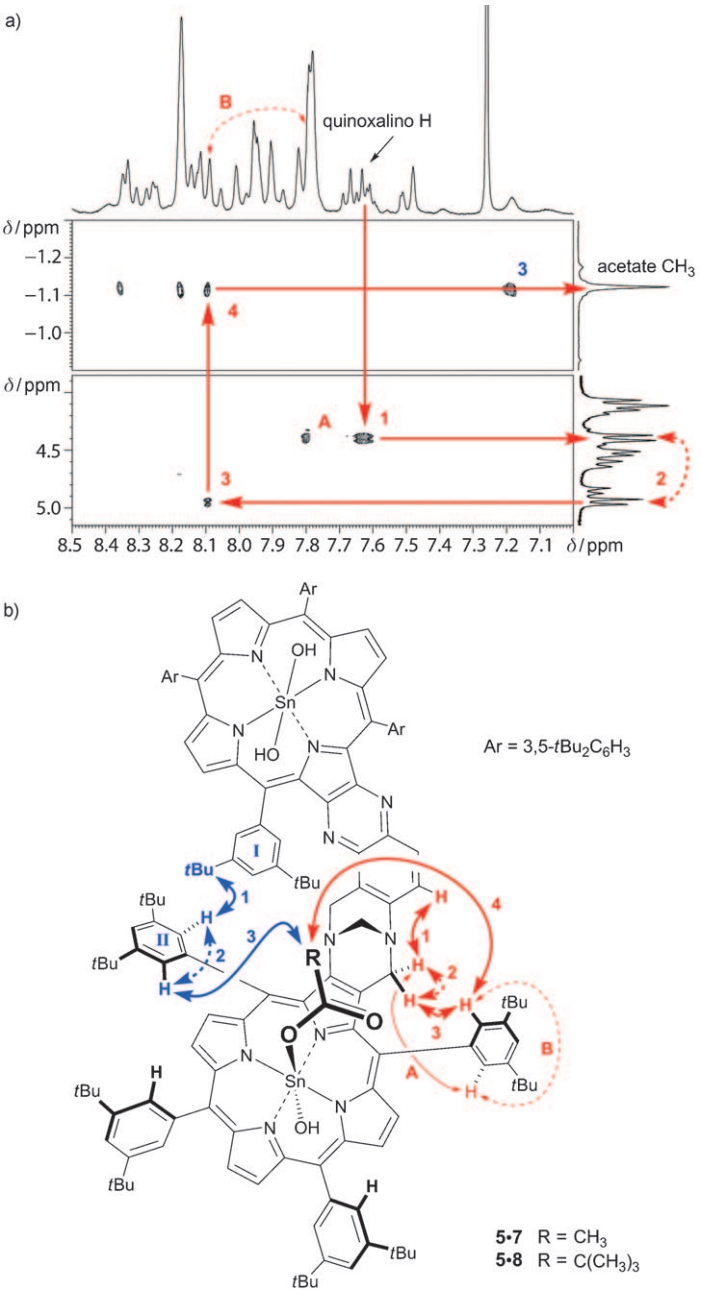

Figure 3. a) ROESY (400 MHz, $CDCl_3$, 250 K) spectrum showing one pathway of connectivity (red arrows) that allows assignment of the position at which the first molar equivalent of **7** binds to host **5**, forming **5·7** (see red arrows in part b). Dashed arrows indicate spin-coupling. b) Diagrammatic representation of the NOE (solid arrows) and spin-coupled (dashed arrows) connectivity for **5·7** and **5·8** that identify the initial site of complexation. Red indicates pathway one and blue indicates pathway two (see text). Arrows and symbols in part b correspond to those in part a. The **I** ring is the cavity aryl group defined in Figure 1.

in Figure 3b. NOE connectivity (interaction 1 (blue) in Figure 3) to one of the *tert*-butyl groups appended to the cavity aryl group (**I** ring, identified by its NOE connectivity to the cavity aryl proton) allows identification of the signal arising from a **II** ring *ortho* proton. DQF-COSY (interaction 2 (blue) in Figure 3) distinguishes the interior and exterior

cavity *ortho* protons on the B ring and subsequent NOE connectivity (interaction 3 in Figure 3) defines the position of the guest ligands on the asymmetric host **5** surface. The bound ligand also connects through NOE to the other two *ortho* protons on the same face of the porphyrin macrocycle indicated in Figure 3.

Together these two paths of connectivity can only be explained by the binding of ligands at the exterior face of the porphyrin. Measurements, in the crystal structure, of the distances between the host nuclei identified in these experiments were also in good agreement with the connectivities determined by ROESY. The next section describes control experiments that allow rationalisation of the factors leading to this binding selectivity.

Factors that determine binding selectivity: We discussed above, in light of the crystal structure data for host **5**, the steric environment at each of the binding sites and the presence of a shallow cavity at one face of the host. We have also drawn attention to the electronic differences between porphyrins and quinoxalinoporphyrins.[18,24] The following series of experiments specifically identifies the importance of each of these factors.

Steric influences: Addition of ≥ 4 molar equivalents of guests **6**, **7** and **8** to host **5** results in ligand exchange at all four binding sites on the host to form the di[dicarboxylatotin(IV)] complexes of host **5**. The di[diformatotin(IV)] and di[diacetatotin(IV)] complexes form within 15 and 30 min, respectively, upon addition of six molar equivalents **6** or **7**. It is not possible, however, to form the di[dipivalatotin(IV)] complex in quantitative yield under these conditions. Addition of eight molar equivalents of **8** to host **5** and a reaction time of 36 h results in the formation of a mixture comprised of the di[dipivalatotin(IV)] complex and only one of the four possible dipivalatotin(IV)–hydroxopivalatotin(IV) complexes (hereafter referred to as the 3:1 complex). ^{1}H–^{119}Sn HMQC of the mixture, depicted in Figure 4d, allows detection of a single hydroxopivalatotin(IV) nucleus along with two dipivalatotin(IV) nuclei. The dipivalatotin(IV) nucleus of the 3:1 complex is coincident with those signals for the di[dipivalatotin(IV)] complex.

This result shows that the steric environment at one of the binding sites offers a significant deterrent to ligand exchange for **8**, the bulkiest of the carboxylate guests. From the crystal structure analysis for host **5** (Figure 1) it is clear that this hindered binding site is that on the interior cavity position of the porphyrin, which is partially obscured by the cavity aryl group identified in Figure 1b. Complete di[dipivalatotin(IV)] complex formation does not occur because steric interaction at this binding site results in mechanical strain in the tin(IV)–pivalato bond, activating it to hydrolysis by water released during binding.

Examination of the chemical shifts for the cavity aryl proton (identified in Figure 1 by the orange arrows) in the di[dicarboxylatotin(IV)] complexes shows that as ligands increase in steric demand from hydroxo, through formato and acetato to pivalato, there is increasing downfield shift in the resonance for this proton that correlates with the steric demand of the ligand, see Figure 5. This is consistent with steric interaction between the bound ligand and the cavity aryl group and displacement of the cavity aryl proton away from the major shielding zone of the porphyrin macrocycle. The chemical shift for the cavity aryl proton in the 3:1 complex is very similar to that in host **5**, which indicates that in this complex this binding site maintains a hydroxo ligand. The proximity of the cavity aryl proton to this binding site was also detected by ROESY experiments on host **5**.[26] Together these experiments clearly show the steric impedance to ligand exchange at the interior cavity site of the porphyrin macrocycle.

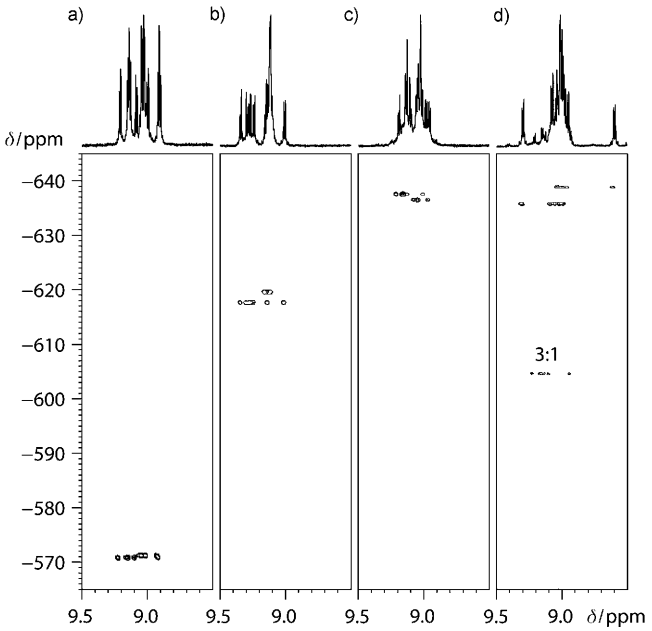

Figure 4. ^{1}H–^{119}Sn HMQC (400 MHz, $CDCl_3$, 300 K) showing expansions of the β-pyrrolic proton region. a) Host **5**. b) Host **5**+6.0 molar equivalents **6**, 15 min, di[diformatotin(IV)] complex. c) Host **5**+6.0 molar equivalents **7**, 30 min, di[diacetatotin(IV)] complex. d) Host **5**+8.0 molar equivalents **8**, 36 h, di[dipivalatotin(IV)] complex and one isomer of the 3:1 pivalato–host complex.

Macrocyclic electronic structure influences: The effect of the electronic differences between the porphyrin and quinoxalinoporphyrin macrocycles of host **5** on ligand exchange rates was tested in such a way as to control the morphology of the host. The binding of **7** to a 1:1 molar ratio of model compounds dihydroxotin(IV) porphyrin **9a**[21] and dihydroxotin(IV) quinoxalinoporphyrin **10a**[21] was examined by employing concentrations such that the NMR spectroscopy titration experiment was precisely analogous to those performed on host **5**.

This ^{1}H NMR spectroscopy titration, depicted in Figure 6, shows that the presence of the quinoxalino group at the porphyrin periphery significantly reduces the rate of ligand exchange at the tin(IV) centre. The electron-withdrawing effect of the quinoxalino group increases the Lewis acidity

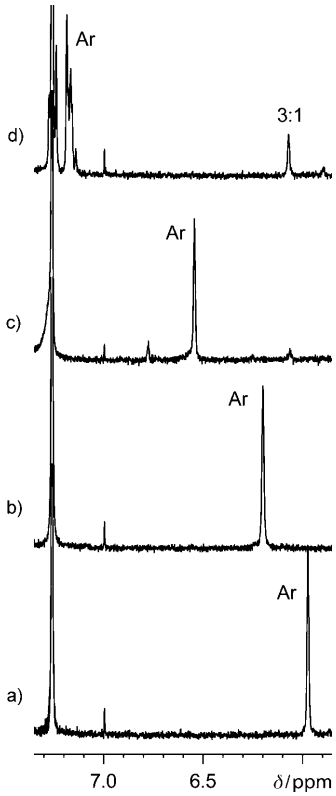

Figure 5. ^{1}H NMR spectrum (400 MHz, $CDCl_3$, 300 K) for the cavity aryl proton (Ar) defined in Figure 1. a) Host **5**. b) Host **5**+6.0 molar equivalents **6**, 15 min, di[diformatotin(IV)] complex. c) Host **5** +6.0 molar equivalents **7**, 30 min, di[diacetatotin(IV)] complex. d) Host **5**+8.0 molar equivalents **8**, 36 h di[dipivalatotin(IV)] complex and one isomer of the 3:1 pivalato–host complex (3:1). Note the downfield shift with the increasing steric demand of the ligands. The 3:1 complex maintains a hydroxo ligand adjacent to the cavity aryl group.

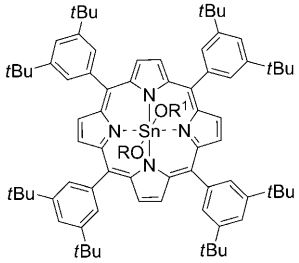

9a: R = R^1 = H
9b: R = H R^1 = $COCH_3$
9c: R = R^1 = $COCH_3$

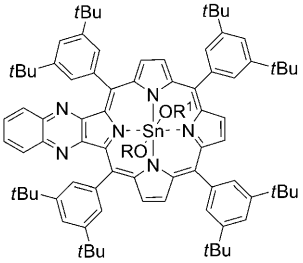

10a: R = R^1 = H
10b: R = H R^1 = $COCH_3$
10c: R = R^1 = $COCH_3$

of the tin(IV) metal centre, thereby reducing the basicity of the hydroxo ligand oxygen (the hydrogen-bond acceptor in the initial stage of acidolysis) and strengthening the hydroxo ligand bond to the tin(IV) metal centre. As a result, ligand exchange kinetics are more rapid at the porphyrin tin(IV) centre and these sites bind the majority of the initial aliquot of carboxylic acid guest.

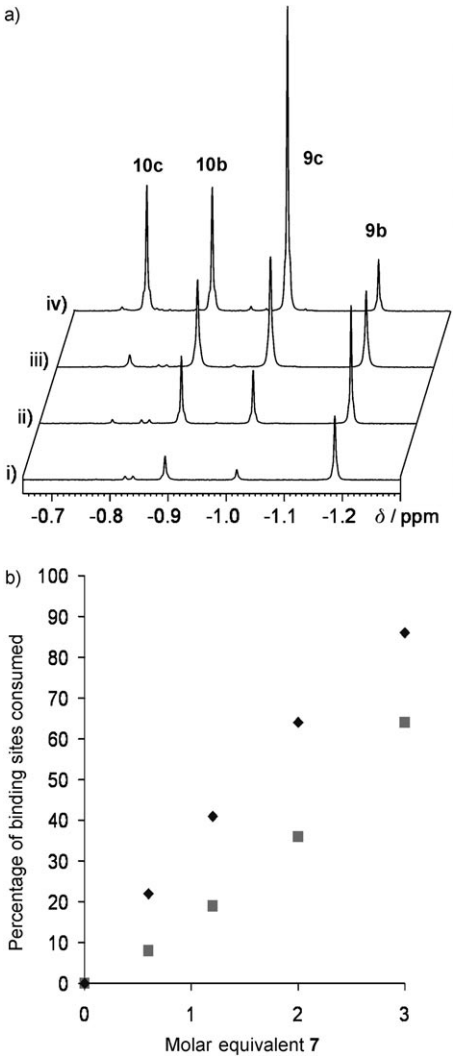

Figure 6. a) ^{1}H NMR (400 MHz, $CDCl_3$, 300 K) titration of a 1:1 molar ratio mixture of **9** and **10** with **7**. i) 0.6, ii) 1.2, iii) 2.0 and iv) 3.0 equivalents **7**. Each acetate environment was identified by ^{1}H–^{119}Sn HMQC. b) Plot showing the proportion of binding site consumed on **9** (◆) and **10** (■) after each addition of aliquot and 30 min binding time.

Hydrogen-bonding mode: The experiments described above show a clear influence on the rate of ligand exchange at binding sites on host **5** by both steric factors and the electron-withdrawing effect of the fused quinoxaline group. These factors work in concert to direct the first molar equivalent aliquot of monodentate carboxylic acid guest to bind at their preferred site, the exterior, sterically non-congested site on the electronically favoured porphyrin macrocycle. However, these factors are overridden in the binding of dicarboxylic acid guests of appropriate length to bridge the two tin(IV) centres across the interior of the cavity.

Adipic acid **11** and subaric acid **12** form ditopic hydrogen-bond interactions with host **5** between the intracavity hydroxo ligands in the initial stage of the ligand exchange process. This organises the guest into a regioselective interaction with the tetravalent host, which is detected by ^{1}H NMR spectroscopy (see Figure 5b and Figure S9b in the Support-

ing Information). The guest is then trapped to the host in this orientation by tin(IV)–carboxylate bond formation. This exclusive intracavity binding may be predicted by the "molecular ruler" concept.[22] At completion of ditopic binding the methanodiazocine bridge region of the ^{1}H NMR spectrum simplifies to six geminally coupled doublets, indicative that there is one host–guest complex in solution (See Figure 7c inset and Figure S9c, inset in the Supporting Information).

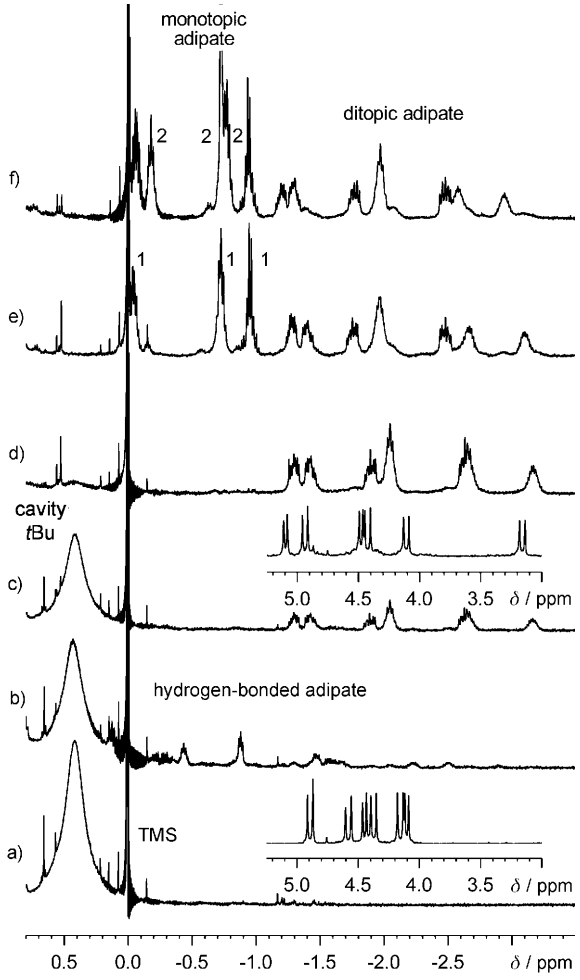

Figure 7. ^{1}H NMR (400 MHz, $CDCl_3$, 300 K) spectrum showing the binding of **11** to host **5**. a) Host **5**. Inset shows the methanodiazocine bridge region. b) Host **5**+0.4 molar equivalents **11**, 30 min. c) Host **5**+0.4 equivalents **11**, 17 h. Inset shows methanodiazocine bridge region, six doublets of a single complex. d) Host **5**+0.9 equivalents **11**, 17 h. e) Host **5**+2.0 equivalents **11**, 1 h. f) Host **5**+3.0 equivalents **11**, 10 h. The C5-methylene for external adipate is obscured beneath the *t*Bu signals. 1 and 2, see text for explanation.

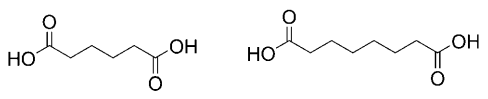

11

12

The binding of **11** and **12** subjects them to the asymmetric environment of the host **5** cavity. In this environment each of the methylene protons of the aliphatic backbone are non-equivalent and give rise to complex splitting patterns in the ^{1}H NMR spectrum. For **11** these eight resonances are clearly resolved in the upfield region of the spectrum typical for binding modes between porphyrin centres,[5] see Figure 7d. As subsequent aliquots of **11** and **12** are added, binding occurs at the exterior of the host. Guests bound at the exterior are also subject to a non-symmetric environment, but rapid rotation about methylene–methylene bonds reduces dispersion of the signals for the diastereotopic protons appended to each carbon. The signals for the interior and exterior bound ligands are readily identified by chemical shift.

The electronic effect differences between the porphyrin and the quinoxalinoporphyrin identified in the previous section are also evident in the titration of **11** and **12** with host **5**. When the second molar equivalent aliquot of diacid is added to host **5**, one major set of external bound-ligand signals appears. Addition of the third molar equivalent aliquot results in appearance of a second set of externally bound ligand signals 0.1 to 0.2 ppm upfield of the original signals, which indicates that ligand exchange is favoured at one of the exterior cavity sites, most likely that at the exterior face of the porphyrin macrocycle. See signals marked 1 and 2 in Figure 7e and f and Figure S9 in the Supporting Information.

These experiments with dicarboxylic acids **11** and **12** show that while the steric and electronic influences on monodentate ligand binding are significant, these are overcome by guests that possess the facility to form ditopic hydrogen bonds between the interior cavity hydroxo ligands in the initial stage of the ligand exchange process. This ditopic hydrogen-bonding mode represents the thermodynamic product of the pre-equilibrium and essentially renders the first tin(IV)–carboxylate bond formation to be an intramolecular process, resulting in the rapid kinetic trapping of this mode of interaction.

Conclusion

Steric and electronic influences and the operation of cavity effects are shown to result in exquisite control over hydrogen-bonding propensity, ligand exchange, and hence, carboxylate binding to a tetravalent di[dihydroxotin(IV)] bis-porphyrin host (**5**) designed to identify the significance of these factors. These steric, electronic and cavity-effect properties operate by influencing the kinetics and/or thermodynamics of hydrogen-bond interactions in the pre-equilibrium to ligand exchange. Ligand exchange may then proceed from this dynamic hydrogen-bonded mode of interaction with dissociation of a molecule of water and tight binding of the oxygen anion at the tin(IV) centre, siphoning material out of the hydrogen-bond pre-equilibrium to yield a tin(IV)-bound complex that reflects the incidence of favoured interactions established by hydrogen bonding. This results in the

facility for simple carboxylic acid guests to bind with significant site specificity on the asymmetric surface of host **5**.

It is worth noting that all of the information required to direct this regioselective binding at host **5** was installed with a single facile condensation of **1** and **2** with formaldehyde to generate the methanodiazocine Tröger's base linker between the macrocycles. The Tröger's base condensation of these two achiral and electronically distinct arylamines defines the steric environment at each binding site, the presence of the cavity, the rigidity and the asymmetry of the host.

This work shows there is potential for expanding the application of tin(IV) porphyrins in the generation of molecular devices, beyond the formation of complexes that are symmetrical about the six-coordinate tin(IV) metal centre. Tuning the outcome of the hydrogen-bond pre-equilibrium to ligand exchange and kinetic trapping of this mode of interaction offers chemoselective and regioselective binding of oxygen anions at the tin(IV) centre as well as covalent strength association.

Experimental Section

General procedures: ^{1}H NMR spectra were recorded on a Bruker DPX-400 (400 MHz) spectrometer and signals are quoted in ppm relative to the residual protiated solvent peak.[27] The 2D NMR spectra discussed were recorded on the same instrument by using standard Bruker pulse programs. Temperature was controlled by using a Bruker B-VT 2000 variable temperature unit. ^{119}Sn NMR (149 MHz) chemical shifts are quoted relative to the external standard dihydroxo[5,10,15,20-tetrakis-(3,5-di-*tert*-butylphenyl)porphyrinato]tin(IV) (^{119}Sn = −569.2 ppm)[21] $CDCl_3$ was dried and deacidified by filtration through a plug of anhydrous potassium carbonate and activated neutral alumina prior to use. Other deuteriated solvents were used as received. See the Supporting Information for additional details and routine synthetic procedures.

Synthesis of 4: Freshly prepared **1**[16] (185 mg, 0.170 mmol) and **2**[14] (101 mg, 86.0 μmol) were dissolved in tetrahydrofuran (16 mL) and nitrogen was bubbled through the solution for 10 min. A solution of hydrochloric acid (32% w/v, 2 mL) in ethanol (4 mL) was added and nitrogen was passed over the solution for 10 min. Formaldehyde (37% w/v, 0.45 mL) was added and the reaction was heated at 65 °C under nitrogen for 36 h. The reaction was diluted with diethyl ether (100 mL), washed with water (4 × 100 mL) and the organic solvent was removed. The residue was precipitated from dichloromethane/methanol (1:1) to yield an amorphous purple residue (205 mg) composed of three major products, as determined by TLC (1:1 dichloromethane/light petroleum). The residue was dissolved in chloroform (20 mL) and treated with zinc(II) acetate dihydrate (300 mg, 1.37 mmol) dissolved in methanol (10 mL) at reflux for 5 min and the organic solvents were evaporated to dryness. TLC analysis (1:1 dichloromethane/light petroleum) indicated complete consumption of the starting material. The residue was purified by chromatography over silica (dichloromethane/light petroleum, 1:2). The first major fraction was evaporated to yield dizinc(II) Tröger's base bis-porphyrin[16] (103 mg, 52%) with identical spectral properties as those reported previously. The second major band was collected to yield **3** (37 mg) as a purple residue. This material was not analytically pure, but identification by ^{1}H NMR spectroscopy was possible. ^{1}H NMR (400 MHz, $CDCl_3$, 300 K): δ = −0.23 (br s, 18H; *t*BuH), 1.33 (s, 18H; *t*BuH), 1.38 (s, 9H; *t*BuH), 1.42 (br s, 9H; *t*BuH), 1.44 (s, 9H; *t*BuH), 1.47 (s, 9H; *t*BuH), 1.48 (br s, 9H; *t*BuH), 1.49 (9H; s, *t*BuH), 1.51 (s, 9H; *t*BuH), 1.53 (s, 9H; *t*BuH), 1.56 (s, 18H; *t*BuH), 1.57 (s, 9H; *t*BuH), 1.65 (s, 9H; *t*BuH), 3.99 (d, 1H; J = 18.4 Hz, methylene H), 4.02 (d, 1H; J = 12.4 Hz, methylene H), 4.15 (d, 1H; J = 17.5 Hz, methylene H), 4.46 (d, J = 18.4 Hz, 1H; methylene H), 4.53 (d, J = 12.4 Hz, 1H; methylene H), 4.85 (d, J = 17.5 Hz, 1H; methylene H), 4.96 (dd, J = 1.8 Hz, 1H; Ar H), 7.48 (d, J = 9.2 Hz, 1H; quinoxalino H), 7.53 (dd, J = 1.8 Hz, 1H; Ar H), 7.60 (d, J = 9.2 Hz, 1H; quinoxalino H), 7.72–7.75 (m, 4H; Ar H), 7.77 (dd, J = 1.8 Hz, 1H; Ar H), 7.79 (dd, J = 1.8 Hz, 1H; Ar H), 7.85 (dd, J = 1.8 Hz, 1H; Ar H), 7.88 (dd, J = 1.8 Hz, 1H; Ar H), 7.89 (dd, J = 1.8 Hz, 1H; Ar H), 7.91 (dd, J = 1.8 Hz, 1H, Ar H), 7.96 (br dd, J = 1.8 Hz, 1H; Ar H), 8.08 (dd, J = 1.8 Hz, 1H; Ar H), 8.13 (dd, J = 1.8 Hz, 1H; Ar H), 8.14 (dd, J = 1.8 Hz, 1H; Ar H), 8.17 (dd, J = 1.8 Hz, 1H; Ar H), 8.25 (dd, J = 1.8 Hz, 1H; Ar H), 8.28 (dd, J = 1.8 Hz, 1H; Ar H), 8.41 (d, J = 4.9 Hz, 1H; β-pyrrolic H), 8.70 (d, J = 4.7 Hz, 1H; β-pyrrolic H), 8.77–8.80 (m, 3H; β-pyrrolic H), 8.87 and 8.88 (ABq, J = 4.9 Hz, 2H; β-pyrrolic H), 8.97 (d, J = 4.7 Hz, 1H; β-pyrrolic H), 9.00–9.03 (m, 3H; β-pyrrolic H), 9.07 ppm (d, J = 4.7 Hz, 1H; β-pyrrolic H).

The third major fraction was collected to yield dizinc(II) extended Tröger's base bis-porphyrin[14,17] (53 mg, 48%) with identical spectral properties to those previously reported. Compound **3** (37 mg) was dissolved in dichloromethane (20 mL) and shaken with hydrochloric acid (32% w/v, 10 mL) for 5 min. The organic layer was washed with water (4 × 50 mL) and evaporated. The residue was purified by chromatography over silica (dichloromethane/light petroleum, 1:2). The major band was collected, evaporated to dryness and the residue was recrystallised from dichloromethane/methanol (1:1) to yield **4** as a purple microcrystalline powder (27 mg, 14%). M.p. > 300 °C; ^{1}H NMR (400 MHz, $CDCl_3$, 300 K): δ = −2.49 (br s, 2H; inner NH), −2.21 (br s, 1H; inner NH), −2.17 (br s, 1H; inner NH), −0.14 (br s, 18H; *t*BuH), 1.35 (s, 18H; *t*BuH), 1.39 (s, 9H; *t*BuH), 1.43 (s, 18H; *t*BuH), 1.46 (s, 18H; *t*BuH), 1.51 (br s, 9H; *t*BuH), 1.53–1.54 (m, 36H; *t*BuH), 1.58 (s, 9H; *t*BuH), 1.65 (s, 9H; *t*BuH), 3.89 (d, J = 18.1 Hz, 1H; methylene H), 3.99 (d, J = 12.2 Hz, 1H; methylene H), 4.07 (d, J = 17.4 Hz, 1H; methylene H), 4.20 (br d, J = 18.1 Hz, 1H; methylene H), 4.52 (d, J = 12.2 Hz, 1H; methylene H), 4.74 (d, J = 17.4 Hz, 1H; methylene H), 5.15 (dd, J = 1.5 Hz, 1H; Ar H), 7.37 (d, J = 9.3 Hz, 1H; quinoxalino H), 7.49 (br dd, 2H; Ar H), 7.50 (d, J = 9.3 Hz, 1H; quinoxalino H), 7.55 (dd, J = 1.7 Hz, 1H; Ar H), 7.72 (dd, J = 1.7 Hz, 1H; Ar H), 7.73–7.76 (m, 3H; Ar H), 7.79 (dd, J = 1.7 Hz, 1H; Ar H), 7.84 (dd, J = 1.7 Hz, 1H; Ar H), 7.86–7.87 (m, 2H; Ar H), 7.89–7.90 (m, 3H; Ar H), 7.97 (dd, J = 1.7 Hz, 1H; Ar H), 8.00 (br s, 2H; Ar H), 8.07 (dd, J = 1.7 Hz, 1H; Ar H), 8.14–8.16 (m, 2H; Ar H), 8.30 (dd, J = 1.7 Hz, 1H; Ar H), 8.32 (dd, J = 1.7 Hz, 1H; Ar H), 8.42 (d, J = 5.1 Hz, 1H; β-pyrrolic H), 8.62–8.66 (m, 3H; β-pyrrolic H), 8.72 (d, J = 4.9 Hz, 1H; β-pyrrolic H), 8.81–8.88 (m, 6H; β-pyrrolic H), 8.92 ppm (d, J = 5.1 Hz, 1H; β-pyrrolic H); IR ($CHCl_3$): $\tilde{\nu}$ = 3337 (w), 2964 (s), 2905 (m), 2868 (m), 1593 (s), 1477 (m), 1466 (m), 1458 (m), 1425 (w), 1394 (w), 1364 (m), 1292 (w), 1263 (w), 1248 (m), 1126 (w), 999 (w), 922 (m), 883 cm^{-1} (m); UV/Vis ($CHCl_3$): λ_{max} (log ε): 423 (5.50), 440 sh (5.41), 523 (4.46), 601 (4.12), 650 nm (3.72); MS (ESI): m/z: 2295.38 $[M]^+$; MS (HR-ESI-FT/ICR): m/z: calcd for $C_{161}H_{192}N_{12}+2H^+$: 1148.2785; found: 1148.2740 $[M+2H]^{2+}$.

Synthesis of 5: Bis-porphyrin **4** (20.0 mg, 8.71 μmol) and anhydrous tin(II) chloride (50.0 mg, 0.264 mmol) were combined and pyridine (4 mL) was added. The mixture was heated to reflux with efficient stirring for 12 h. The cooled reaction was diluted with diethyl ether (100 mL), washed with water (4 × 100 mL) and the solvent was evaporated under reduced pressure until there was no trace of pyridine. The residue was purified by chromatography over neutral alumina (class IV, dichloromethane/light petroleum, 1:1) and the major band was collected and evaporated. The residue was dissolved in tetrahydrofuran (100 mL) and a solution of anhydrous potassium carbonate (560 mg, 4.05 mmol) in distilled water was added. The mixture was heated at reflux and stirred efficiently for 12 h, diluted with freshly distilled diethyl ether (100 mL), washed with deionised water (3 × 100 mL), dried over anhydrous sodium sulfate, filtered and evaporated. The residue was recrystallised from freshly distilled dichloromethane/acetonitrile (1:1) to yield **5** as lustrous purple crystals suitable for X-ray crystallography (18 mg, 80%). M.p. > 300 °C; ^{1}H NMR (400 MHz, $CDCl_3$, 300 K): δ = −7.44 (br s, 1H; OH ligand), −7.05 (br s, satellites ^2J(H,Sn) = 36 Hz, 2H; OH ligand), −6.56 (br s, satellites ^2J(H,Sn) = 34 Hz, 1H; OH ligand), 0.43 (br s, 18H; *t*BuH), 1.35 (br s, 18H; *t*BuH), 1.46 (s, 9H; *t*BuH), 1.49 (s, 9H; *t*BuH), 1.499 (s, 9H; *t*BuH), 1.503 (s, 9H; *t*BuH), 1.51 (s, 9H; *t*BuH), 1.54 (s, 9H; *t*BuH), 1.55 (s, 9H; *t*BuH), 1.58 (s, 9H; *t*BuH), 1.59 (s, 9H; *t*BuH), 1.60 (s, 9H; *t*BuH), 1.620 (s, 9H; *t*BuH), 1.626 (s, 9H; *t*BuH), 4.11 (d, J =

12.5 Hz, 1H; methylene H), 4.17 (d, J=18.5 Hz, 1H; methylene H), 4.38 (d, J=17.6 Hz, 1H; methylene H), 4.46 (d, J=12.5 Hz, 1H; methylene H), 4.59 (d, J=18.5 Hz, 1H; methylene H), 4.90 (d, J=17.6 Hz, 1H; methylene H), 5.99 (br dd, J=1.7 Hz, 1H; Ar H), 7.59 (dd, 1.8 Hz, 1H; Ar H), 7.61 (d, J=9.1 Hz, 1H; quinoxalino H), 7.70 (d, J=9.1 Hz, 1H; quinoxalino H), 7.83–7.84 (m, 3H; Ar H), 7.88 (dd, 1.7 Hz, 1H; Ar H), 7.93 (dd, 1.5 Hz, 1H; Ar H), 7.95 (dd, 1.8 Hz, 1H; Ar H), 7.80–7.81 (m, 2H; Ar H), 8.04 (dd, 1.7 Hz, 1H; Ar H), 8.08–8.10 (m, 2H; Ar H), 8.16 (dd, 1.7 Hz, 1H; Ar H), 8.17–8.18 (m, 2H; Ar H), 8.26 (dd, 1.7 Hz, 1H; Ar H), 8.30 (dd, 1.7 Hz, 1H; Ar H), 8.31–8.32 (m, 2H; Ar H), 8.92 (d, J= 4.9 Hz, satellites ^4J(H,Sn) = 10 Hz, 1H; β-pyrrolic H), 8.93 (d, J=4.9 Hz, satellites ^4J(H,Sn) = 10 Hz, 1H; β-pyrrolic H), 8.99–9.07 (m, 5H; β-pyrrolic H), 9.10 (d, J=4.9 Hz, satellites ^4J(H,Sn) = 10 Hz, 1H; β-pyrrolic H), 9.13–9.18 (m, 3H; β-pyrrolic H), 9.22 ppm (d, J=4.6 Hz, satellites ^4J-(H,Sn) = 10 Hz, 1H; β-pyrrolic H); ^{119}Sn NMR (149 MHz, $CDCl_3$, $SnMe_4$): $\delta = -571.3$, -570.9 ppm; IR ($CHCl_3$): $\tilde{\nu}$=3693 (w), 3618 (w), 2964 (s), 2905 (m), 2870 (m), 1593 (s), 1477 (m), 1468 (m), 1427 (m), 1394 (m), 1364 (m), 1344 (w), 1294 (w), 1265 (s), 1248 (m), 1229 (m), 1194 (w), 1169 (w), 1150 (w), 1128 (w), 1055 (w), 1032 (w), 1020 cm^{-1} (w); UV/Vis ($CHCl_3$): λ_{max} ($\log\varepsilon$) = 429 (5.63), 466 (5.38), 565 (4.53), 584 (4.38), 598 (4.36), 640 nm (4.29); MS (ESI): m/z: 1288.8 $[M-OH]^{2+}$; 1281.5 $[M-2OH]^{2+}$; MS (HR-ESI-FT/ICR): m/z: calcd for $C_{161}H_{190}N_{12}O_2Sn_2$: 1281.1614; found: 1281.1619 $[M-2OH]^{2+}$.

^{1}H NMR binding experiments: Host **5** (4 mg, 1.5 μmol) was dissolved in $CDCl_3$ (600 μL, ≈2.5 mM) in 5 mm ID NMR tubes. Standard solutions of carboxylic acid guests **6**, **7** and **8** were prepared in $CDCl_3$ (2.00 mL, ≈0.100 M). Standard solutions of dicarboxylic acid guests **11** and **12** were prepared in [D_6]DMSO/$CDCl_3$ (10:90, 2.00 mL, ≈0.100 M). Precise molar equivalent aliquots of guests **6**–**8**, **11** and **12** were added to host **5** by microlitre syringe and the mixture was immediately stirred. Monitoring by ^{1}H NMR spectroscopy then commenced (≤2 min post aliquot addition) and continued until a cessation in spectral changes indicated binding had reached equilibrium. Further characterisation by the NMR spectroscopy techniques indicated was then performed on these equilibrium systems.

CCDC-699388 contains the supplementary crystallographic data for this paper. These data can be obtained free of charge from The Cambridge Crystallographic Data Centre via www.ccdc.cam.ac.uk/data_request/cif.

Acknowledgements

We thank the Australian Research Council for a Discovery Grant (DP A00106402) to M.J.C. and The University of Sydney for an H. B. and F. M. Gritton Postgraduate Award to PRB.

[1] a) C. B. Anfinsen, *Science* **1973**, *181*, 223–230; b) K. Pauwels, I. Van Molle, J. Tommassen, P. Van Gelder, *Mol. Microbiol.* **2007**, *64*, 917–922; c) G. D. Rose, P. J. Fleming, J. R. Banavar, A. Maritan, *Proc. Natl. Acad. Sci. USA* **2006**, *103*, 16623–16633; d) A. M. Stanley, K. G. Fleming, *Arch. Biochem. Biophys.* **2008**, *469*, 46–66.

[2] a) J. M. West, H. Tsuruta, E. R. Kantrowitz, *J. Biol. Chem.* **2002**, *277*, 47300–47304; b) G. F. Sánchez-Pérez, M. Gasset, J. J. Calvete, M. A. Pajares, *J. Biol. Chem.* **2003**, *278*, 7285–7293; c) M. J. Lindberg, J. Normark, A. Holmgren, M. Oliveberg, *Proc. Natl. Acad. Sci. USA* **2004**, *101*, 15893–15898.

[3] a) A. Petitjean, L. A. Cuccia, M. Schmutz, J.-M. Lehn, *J. Org. Chem.* **2008**, *73*, 2481–2495; b) E. S. Barrett, T. J. Dale, J. Rebek, Jr., *J. Am. Chem. Soc.* **2008**, *130*, 2344–2350; c) S.-S. Li, H.-J. Yan, L.-J. Wan, H.-B. Yang, B. H. Northrop, P. J. Stang, *J. Am. Chem. Soc.* **2007**, *129*, 9268–9269; d) D. Ajami, J. Rebek, Jr., *Proc. Natl. Acad. Sci. USA* **2007**, *104*, 16000–16003; e) H.-B. Yang, K. Ghosh, B. H. Northrop, Y.-R. Zheng, M. M. Lyndon, D. C. Muddiman, P. J. Stang, *J. Am. Chem. Soc.* **2007**, *129*, 14187–14189; f) E. A. Katayev, N. V. Boev, V. N. Khrustalev, Y. A. Ustynyuk, I. G. Tananaev, J. L. Sessler, *J. Org. Chem.* **2007**, *72*, 2886–2896; g) H.-B. Yang, A. M. Hawkridge, S. D. Huang, N. Das, S. D. Bunge, D. C. Muddiman, P. J. Stang, *J. Am. Chem. Soc.* **2007**, *129*, 2120–2129; h) K. A. Nielsen, W.-S. Cho, G. H. Sarova, B. M. Petersen, A. D. Bond, J. Becher, F. Jensen, D. M. Guldi, J. L. Sessler, J. O. Jeppesen, *Angew. Chem.* **2006**, *118*, 7002–7007; *Angew. Chem. Int. Ed.* **2006**, *45*, 6848–6853; i) J. M. Rodriguez, A. D. Hamilton, *Angew. Chem.* **2007**, *119*, 8768–8771; *Angew. Chem. Int. Ed.* **2007**, *46*, 8614–8617; j) J. Jayawickramarajah, D. M. Tagore, L. K. Tsou, A. D. Hamilton, *Angew. Chem.* **2007**, *119*, 7727–7730; *Angew. Chem. Int. Ed.* **2007**, *46*, 7583–7586.

[4] a) F. Bulos, S. L. Roberts, R. L. E. Furlan, J. K. M. Sanders, *Chem. Commun.* **2007**, 3092–3093; b) P. T. Corbett, J. K. M. Sanders, S. Otto, *Angew. Chem.* **2007**, *119*, 9014–9017; *Angew. Chem. Int. Ed.* **2007**, *46*, 8858–8861; c) R. F. Ludlow, J. Liu, H. Li, S. L. Roberts, J. K. M. Sanders, S. Otto, *Angew. Chem.* **2007**, *119*, 5864–5866; *Angew. Chem. Int. Ed.* **2007**, *46*, 5762–5764; d) S. Ulrich, J.-M. Lehn, *Angew. Chem.* **2008**, *120*, 2272–2275; *Angew. Chem. Int. Ed.* **2008**, *47*, 2240–2243.

[5] P. R. Brotherhood, R. A.-S. Wu, P. Turner, M. J. Crossley, *Chem. Commun.* **2007**, 225–227.

[6] H. J. Jo, S. H. Jung, H.-J. Kim, *Bull. Korean Chem. Soc.* **2004**, *25*, 1869–1873.

[7] S. J. Langford, M. A.-P. Lee, K. J. Macfarlane, J. A. Weigold, *J. Inclusion Phenom. Macrocyclic Chem.* **2001**, *41*, 135–139.

[8] S. J. Langford, C. P. Woodward, *CrystEngComm* **2007**, *9*, 218–221.

[9] a) J. E. Redman, N. Feeder, S. J. Teat, J. K. M. Sanders, *Inorg. Chem.* **2001**, *40*, 2486–2499; b) J. C. Hawley, N. Bampos, J. K. M. Sanders, *Chem. Eur. J.* **2003**, *9*, 5211–5222; c) V. F. Slagt, P. W. N. M. van Leeuwen, J. N. H. Reek, *Dalton Trans.* **2007**, 2302–2310; d) A. Guenet, E. Graf, N. Kyritsakas, L. Allouche, M. W. Hosseini, *Chem. Commun.* **2007**, 2935–2937; e) Y. Kim, M. F. Mayer, S. C. Zimmerman, *Angew. Chem. Int. Ed.* **2003**, *42*, 1121–1126; f) K. P. Ghiggino, J. A. Hutchison, S. J. Langford, M. J. Latter, M. A.-P. Lee, P. R. Lowenstern, C. Scholes, M. Takezaki, B. E. Wilman, *Adv. Funct. Mater.* **2007**, *17*, 805–813; g) G. D. Fallon, S. J. Langford, M. A.-P. Lee, E. Lygris, *Inorg. Chem. Commun.* **2002**, *5*, 715–718; h) Y. Tong, D. G. Hamilton, J.-C. Meillon, J. K. M. Sanders, *Org. Lett.* **1999**, *1*, 1343–1346; i) S. J. Langford, M. J. Latter, J. Beckmann, *Inorg. Chem. Commun.* **2005**, *8*, 920–923; j) H. Iwamoto, K. Hori, Y. Fukazawa, *Tetrahedron* **2006**, *62*, 2789–2798; k) G. D. Fallon, M. A.-P. Lee, S. J. Langford, P. J. Nichols, *Org. Lett.* **2002**, *4*, 1895–1898; l) H.-J. Kim, H. J. Jo, J. Kim, S.-Y. Kim, D. Kim, K. Kim, *CrystEngComm* **2005**, *7*, 417–420; m) S. Nimri, E. Keinan, *J. Am. Chem. Soc.* **1999**, *121*, 8978–8982.

[10] a) D. R. Reddy, B. G. Maiya, *J. Porphyrins Phthalocyanines* **2002**, *6*, 3–11; b) H. J. Kim, K.-M. Park, T. K. Ahn, S. K. Kim, K. S. Kim, D. Kim, H.-J. Kim, *Chem. Commun.* **2004**, 2594–2595; c) J. H. Jang, K.-S. Jeon, S. Oh, H.-J. Kim, T. Asahi, H. Masuhara, M. Yoon, *Chem. Mater.* **2007**, *19*, 1984–1991; d) P. P. Kiran, D. R. Reddy, B. G. Maiya, A. K. Dharmadhikari, G. R. Kumar, D. N. Rao, *Opt. Commun.* **2005**, *252*, 150–161; e) D.-M. Ren, Z. Guo, F. Du, Z.-F. Liu, Z.-C. Zhou, X.-Y. Shi, Y.-S. Chen, J.-Y. Zheng, *Int. J. Mol. Sci.* **2008**, *9*, 45–55; f) J. H. Jang, H. J. Kim, H.-J. Kim, C. H. Kim, T. Joo, D. W. Cho, M. Yoon, *Bull. Korean Chem. Soc.* **2007**, *28*, 1967–1972; g) H. Wang, Y. Song, C. J. Medforth, J. A. Shelnutt, *J. Am. Chem. Soc.* **2006**, *128*, 9284–9285; h) Z. Wang, C. J. Medforth, J. A. Shelnutt, *J. Am. Chem. Soc.* **2004**, *126*, 16720–16721; i) J. Fortage, E. Göransson, E. Blart, H.-C. Becker, L. Hammarström, F. Odobel, *Chem. Commun.* **2007**, 4629–4631; j) H. J. Kim, J. H. Jang, H. Choi, T. Lee, J. Ko, M. Yoon, H.-J. Kim, *Inorg. Chem.* **2008**, *47*, 2411–2415.

[11] J. C. Hawley, N. Bampos, R. J. Abraham, J. K. M. Sanders, *Chem. Commun.* **1998**, 661–662.

[12] D. P. Arnold, E. A. Morrison, J. V. Hanna, *Polyhedron* **1990**, *9*, 1331–1336.

[13] M. J. Crossley, L. G. Mackay, A. C. Try, *J. Chem. Soc. Chem. Commun.* **1995**, 1925–1927.

[14] M. J. Crossley, A. C. Try, R. Walton, *Tetrahedron Lett.* **1996**, *37*, 6807–6810.

[15] M. J. Crossley, P. J. Sintic, J. A. Hutchison, K. P. Ghiggino, *Org. Biomol. Chem.* **2005**, *3*, 852–865.

[16] M. J. Crossley, T. W. Hambley, L. G. Mackay, A. C. Try, R. Walton, *J. Chem. Soc. Chem. Commun.* **1995**, 1077–1079.
[17] J. N. H. Reek, A. P. H. J. Schenning, A. W. Bosman, E. W. Meijer, M. J. Crossley, *Chem. Commun.* **1998**, 11–12.
[18] K. M. Kadish, W. E, P. J. Sintic, Z. Ou, J. Shao, K. Ohkubo, S. Fukuzumi, L. J. Govenlock, J. A. McDonald, A. C. Try, Z.-L. Cai, J. R. Reimers, M. J. Crossley, *J. Phys. Chem. B* **2007**, *111*, 8762–8774.
[19] A. D. Adler, F. R. Longo, F. Kampas, J. Kim, *J. Inorg. Nucl. Chem.* **1970**, *32*, 2443–2445.
[20] P. Rothemund, A. R. Menotti, *J. Am. Chem. Soc.* **1948**, *70*, 1808–1812.
[21] M. J. Crossley, P. Thordarson, R. A.-S. Wu, *J. Chem. Soc. Perkin Trans. 1* **2001**, 2294–2302.
[22] M. J. Crossley, P. Thordarson, *Angew. Chem.* **2002**, *114*, 1785–1788; *Angew. Chem. Int. Ed.* **2002**, *41*, 1709–1712.
[23] K. J. Cross, M. J. Crossley, *Aust. J. Chem.* **1992**, *45*, 991–1004.
[24] a) S. Fukuzumi, K. Ohkubo, W. E, Z. Ou, J. Shao, K. M. Kadish, J. A. Hutchison, K. P. Ghiggino, P. J. Sintic, M. J. Crossley, *J. Am. Chem. Soc.* **2003**, *125*, 14984–14985; b) K. M. Kadish, W. E, Z. Ou, J. Shao, P. J. Sintic, K. Ohkubo, S. Fukuzumi, M. J. Crossley, *Chem. Commun.* **2002**, 356–357; c) Z. Ou, K. M. Kadish, W. E, J. Shao, P. J. Sintic, K. Ohkubo, S. Fukuzumi, M. J. Crossley, *Inorg. Chem.* **2004**, *43*, 2078–2086; d) Z. Ou, W. E, J. Shao, P. L. Burn, C. S. Sheehan, R. Walton, K. M. Kadish, M. J. Crossley, *J. Porphyrins Phthalocyanines* **2005**, *9*, 142–151.
[25] a) D. P. Arnold, E. R. T. Tiekink, *Polyhedron* **1995**, *14*, 1785–1789; b) D. P. Arnold, J. P. Bartley, *Inorg. Chem.* **1994**, *33*, 1486–1490; c) G. Smith, D. P. Arnold, C. H. L. Kennard, T. C. W. Mak, *Polyhedron* **1991**, *10*, 509–516; d) D. P. Arnold, *Polyhedron* **1988**, *7*, 2225–2227; e) D. P. Arnold, *J. Chem. Educ.* **1988**, *65*, 1111–1112.
[26] P. R. Brotherhood, I. J. Luck, M. J. Crossley, *Magn. Reson. Chem.* **2008**, DOI: 10.1002/mrc.2356.
[27] H. E. Gottlieb, V. Kotlyar, A. Nudelman, *J. Org. Chem.* **1997**, *62*, 7512–7515.

Received: August 28, 2008
Published online: November 4, 2008

